SUBMITTED TO:

DEPARTMENT OF ENERGY
1000 INDEPENDENCE AVENUE, SW
WASHINGTON, DC

Rights in Data – SBIR/STTR Program

SBIR PHASE II FINAL REPORT

SOLAR DESALINATION FOR MID-SIZED APPLICATIONS

AUGUST 8, 2007 TO AUGUST 7, 2009

SUBMITTED: OCTOBER 20, 2010

GRANT NO. DE-FG02-06ER84525

SUBMITTED BY:

Dr. Andrew Lowenstein, Principal Investigator
AIL RESEARCH, INC.
P.O. BOX 3662
PRINCETON, NJ 08543

SBIR RIGHTS NOTICE (JUN 1987)

These SBIR data are furnished with SBIR rights under Grant No. DE-FG02-06ER84525. For a period of 4 years after acceptance of all items to be delivered under this grant, the Government agrees to use these data for Government purposes only, and they shall not be disclosed outside the Government (including disclosure for procurement purposes) during such period without permission of the grantee, except that, subject to the foregoing use and disclosure prohibitions, such data may be disclosed for use by support contractors. After the aforesaid 4-year period the Government has a royalty-free license to use, and to authorize others to use on its behalf, these data for Government purposes, but is relieved of all disclosure prohibitions and assumes no liability for unauthorized use of these data by third parties. This Notice shall be affixed to any reproductions of these data in whole or in part.

Solar Desalination Technology for Mid-Sized Applications

Summary

Secure sources of clean, freshwater are essential to the welfare of communities throughout the world. Unfortunately, both in this country and abroad, freshwater supplies are increasingly being contested. Faced with threats to growth, economic development and the health of their citizens, governments are battling over the rights to freshwater supplies. These conflicts would be eased or entirely eliminated if a low-cost process for purifying seawater and brackish that relied on a renewable energy resource was available.

Two novel technologies that could become part of a low-cost thermal desalination system were successfully proven in the reported work. One technology efficiently converts solar energy into atmospheric pressure steam, and the other uses atmospheric pressure steam to purify seawater or brackish water.

Diffusion-Gap (DG) Distillation—one of the novel processes that is reported here—falls within a class of desalination technologies referred to as Humidification/Dehumidification (Hum/Dehum) systems. In a hum/dehum system, air at atmospheric pressure is first humidified using seawater and then pure water is condensed from the humid air. In the more efficient hum/dehum systems, the heat released as the water vapor condenses is returned to the process to produce more humid air.

As shown in Figure S1, a DG system consists of a set of extruded plastic plates that have internal

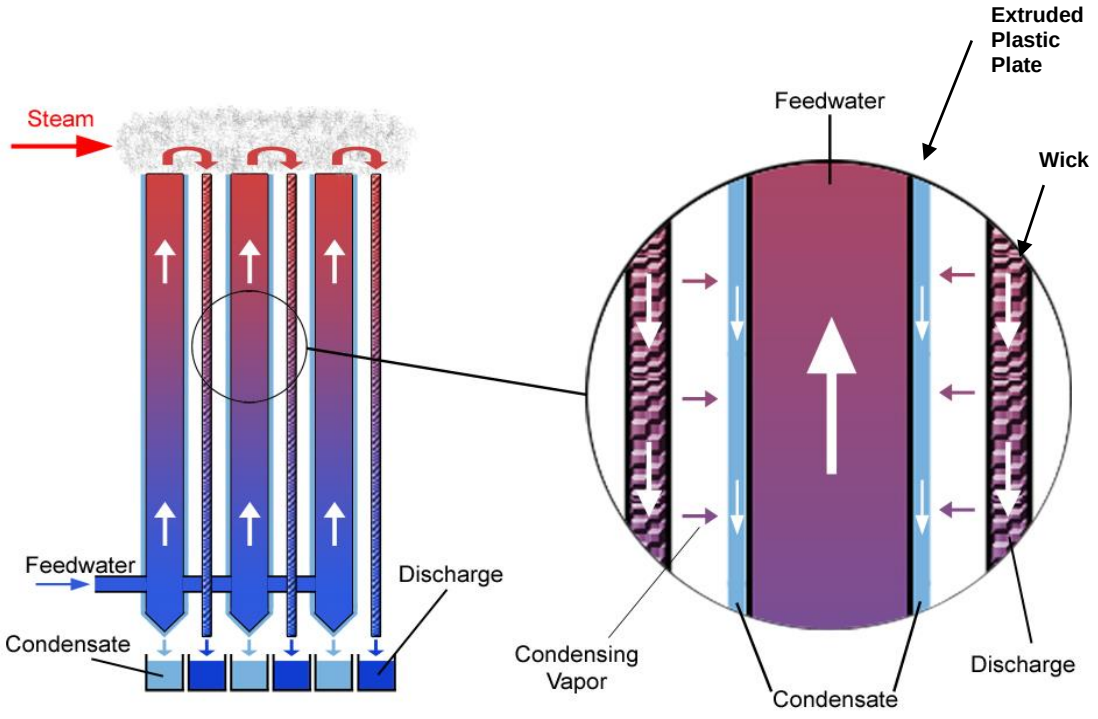

Figure S1 - Schematic of a Diffusion-Gap System

passages and a set of wicking surfaces that are positioned in the gaps between the plates. The brine feed enters at the bottom of each plate, flows upward within the plate, and leaves at the top. As the brine feed flows upward it is preheated by the thermal energy that is released as water vapor condenses on the outer surfaces of the plates. The source of this water vapor is the hot brine that is flowing downward in the wicking surfaces. For the system to operate, the preheated brine that leaves the top of the plates must be further heated before it flows downward in the wicks.

In most applications, the brine's maximum temperature will be less than 100°C. Atmospheric pressure steam generated from natural gas, waste heat or solar thermal energy can then be used to directly heat the brine to its maximum temperature (i.e., the top section of the DG system is flooded with steam, which condenses on the exposed brine, raising its temperature towards 100°C).

The brine flowing in the wicks will cool and become more concentrated as water evaporates from it. However, the downward flowing brine will always be slightly hotter than the upward flowing brine in the section of plate directly across from it. This temperature difference provides the driving force for water vapor to move from the wick to the cooler plate where it condenses. The cooled brine flowing off the wicks and the condensate flowing off the plates are collected in separate troughs.

Unlike conventional thermal separation processes such as multiple-effect boilers and multi-stage flash evaporation, the DG cycle operates at atmospheric pressure. This has the advantage that

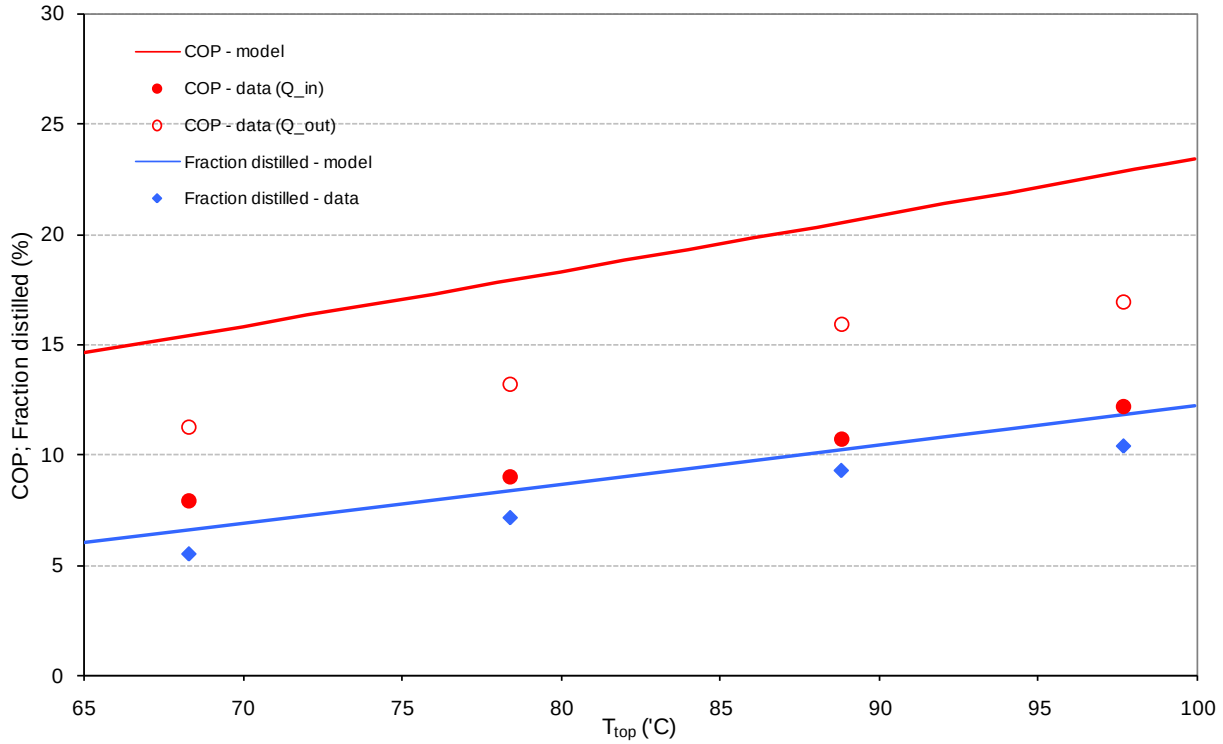

Figure S2 - Performance of 15-Plate Prototype with varying Maximum Temperature

the large vacuum vessels of conventional systems are avoided. Since the partial pressure of the water vapor in the gaps between the plates and the wicks is always less than one atmosphere, the water vapor must diffuse through a background of air. By keeping the air gap very small and by including a large amount of surface area (which is economically feasible because the surface area is inexpensive plastic), the DG cycle can have both a high conversion efficiency and output.

Many of the humidification/dehumidification (HD) cycles proposed by others have the same advantages as the DG cycle: operation at atmospheric pressure and use of plastic heat exchangers. However, alternative HD cycles do not place the evaporating and condensing surfaces in close proximity as is done in the DG cycle. Fans are sometimes used to circulate air between the evaporating and condensing sections, which leads to high requirements for electrical power, or natural circulation is used, which leads to relatively low fluxes of water vapor (and correspondingly large sizes and/or low efficiencies).

A 15-plate model of a DG system was designed, built and successfully tested. The coefficient of performance (COP) shown in Figure S2 is given by the phase-change enthalpy of the distillate divided by the heat input. The solid red points are calculated using the electric power drawn by the heater (that replaces steam as the heat input in this experiment). This COP has a maximum value of about 12.5 for 250 ml/min and T_{max} = 97°C. This does not account for heat losses (about 25 W at T_{max} = 97°C), and therefore provides a low estimate for the performance. A more accurate estimate of performance is obtained by subtracting losses from the heat input, i.e. using the energy leaving the apparatus in the outflow streams for the COP calculation. This COP value is shown in S2 as red circles, having a maximum value of 17 for 250 ml/min and T_{max} = 97°C. This COP is almost twice as high at that achieved in large conventional thermal desalination systems.

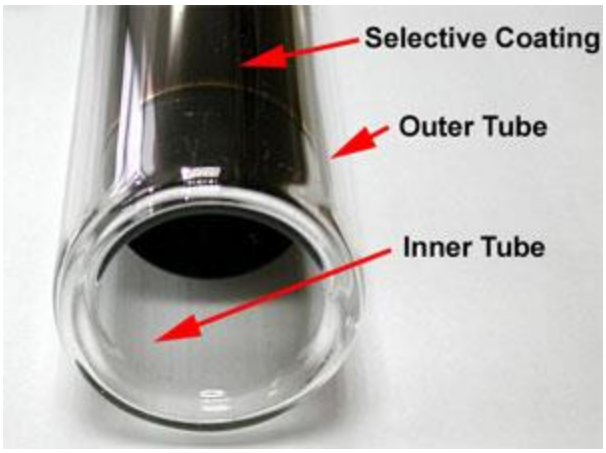

Figure S3 – Evacuated-Tube Dewar-Type Solar Collector

The second major objective of the work reported here was to develop a low-cost solar collector that can provide the thermal energy needed by the desalination system. This objective was met by a novel solar collector that uses the double-wall Dewar tube (essentially vacuum bottles) shown in Figure S3. Each tube is 180 cm in length, and has outer and inner diameters of 5.8 cm and 4.7 cm, respectively. The inner walls of these tubes have a selective absorber coating on the vacuum side that efficiently absorbs visible radiation, but doesn't efficiently reradiate infrared radiation from the hot absorber surface. Solar collection efficiencies are extremely high and stagnation temperatures (i.e., operation without the tubes delivering heat) can exceed 400°F. These tubes are now manufactured in very high volume in China and they can be purchased in the U.S. in quantity for approximately $4 per square foot of absorber area.

For the solar desalination system, the solar source of thermal energy uses the Dewar-tube collectors as simple steam generators. As shown in Figure S4, an array of Dewar tubes is mounted on a level frame. Each tube is connected to a manifold that is fed mineral-free condensate from the output of the desalination plant. The level of water in the manifold

determines the level of water within each tube. At typical operating conditions, steam is quiescently generated from the free surface of water within the tubes as the tubes absorb solar radiation. The steam is collected in the same manifold that delivered water to the tubes.

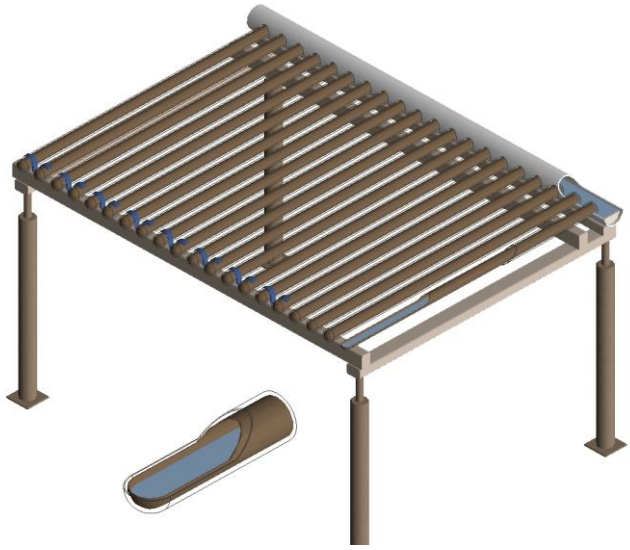

A 24-tube steam generating solar collector was designed and fabricated. A summary of the performance of this prototype is shown in S5. The efficiency is given by the energy value of the steam generated (including preheat, phase change, and superheat components) over the solar radiation absorbed by the collector tubes (not including reflected radiation).

The collector heated up and generated steam on all the test days during the 1½ month test period. Data in Figure S5

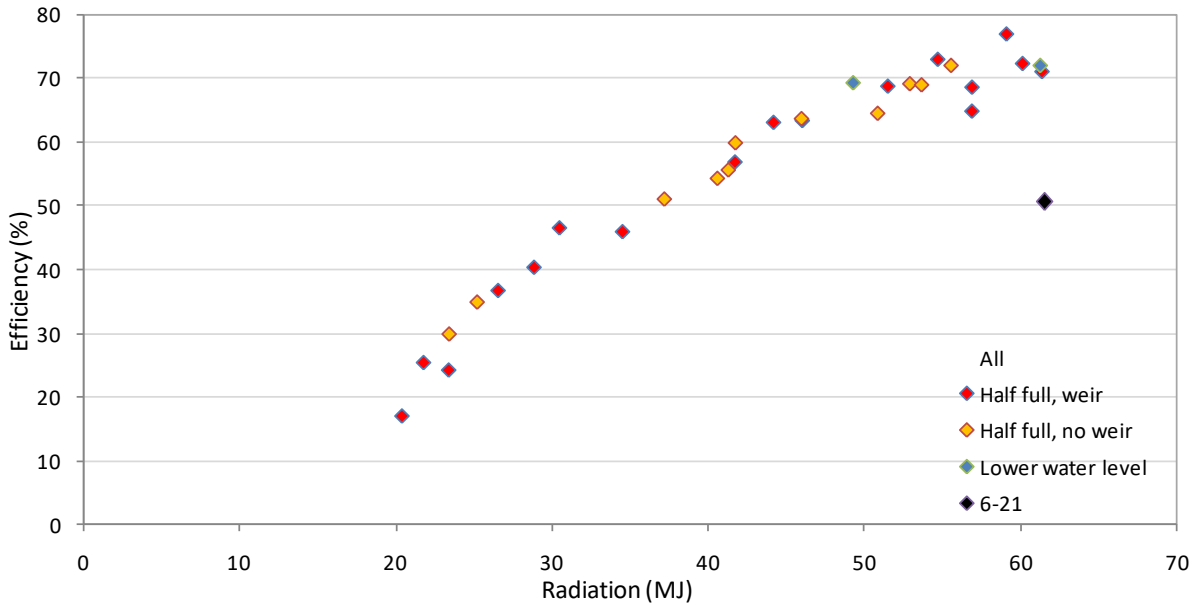

Figure S5 - Efficiency of the 24-tube collector in steam generation, with colored data points indicating variations in tube fill level. Data represents a variety of weather conditions from 6/17/2008 – 7/31/2008.

indicates a clear relationship between radiation and efficiency that is not affected greatly by patterns of insolation, such as variations in cloud cover or haze. The results were also not greatly affected by the water level within the tubes. The blue data points shown in Figure S5 represent days in which the water level was kept at 1/3 full rather than the normal 1/2 full level.

The test data in Figure S5 show that the steam-generating solar collector can convert up to 75% of the solar energy incident on its absorbers into a thermal source of energy for a DG desalination process. This conversion efficiency is comparable to that which can be achieved

with conventional evacuated tube solar collector but (1) the cost to manufacturer the steam-generating collector should be less than one-half that of the conventional collector, and (2) the thermal output from the conventional collector will be hot water that cannot be directly used by the DG system.

An array of steam-generating solar collectors driving a DG desalination unit can meet future needs for sustainable sources of potable water. The technology will be most useful where reverse osmosis in not acceptable either because (1) the cost of electricity is too high, (2) the feedwater has contaminants that would foul the membranes of the reverse-osmosis system, or (3) the application requires water purity that cannot be met by reverse-osmosis.

1.0 Introduction

Secure sources of clean, freshwater are essential to the welfare of communities throughout the world. Unfortunately, both in this country and abroad, freshwater supplies are increasingly being contested. Faced with threats to growth, economic development and the health of their citizens, governments are battling over the rights to freshwater supplies.

Although the first commercial large-scale desalination plants went into operation over 40 years ago, for many communities and industries in need of freshwater, desalination is still too expensive. Furthermore, all commercial desalination is energy intensive. Recent increases in the cost of energy push desalination further beyond the economic grasp of most communities.

Approximately half of the installed base of large desalination plants use some form of thermal distillation. These plants evaporate the brine under vacuum and then condense the water vapor to produce a very pure stream of water. They achieve GORs[1] of 9 or higher by applying the heat released as the water vapor condenses to heat additional brine. This heat transfer occurs across heat exchangers most commonly made from expensive titanium or cupronickel alloys.

Smaller scale thermal desalination plants have been built and operated that use a technology referred to as "humidification/dehumidification" (HD). In these plants, the brine is used to humidify a flow of air. The humid air then flows over a cooled heat exchanger where the water vapor in the air condenses to form the pure product. Since HD plants operate at atmospheric pressure, they commonly use plastic heat exchangers.

The work reported here will both lower the cost for small and mid-sized thermal desalination systems and allow them to run primarily on a renewable energy source, i.e., solar thermal energy.

2.0 Thermal Desalination System – Work Completed

The Diffusion-Gap Process

A novel thermal desalination process was investigated in this project. The geometry of this process leads to the name "Diffusion-Gap Distillation". As shown in Figure 1, the process is implemented with plastic heat exchangers and wicking surfaces. The Diffusion-Gap (DG) system consists of a set of extruded plastic plates that have internal passages and a set of wicking surfaces that are positioned in the gaps between the plates. The brine feed enters at the bottom of each plate, flows upward within the plate, and leaves at the top. As the brine feed flows upward it is preheated by the thermal energy that is released as water vapor condenses on the outer surfaces of the plates. The source of this water vapor is the hot brine that is flowing downward in the wicking surfaces. For the system to operate, the preheated brine that leaves the top of the plates must be further heated before it flows downward in the wicks.

In most applications, the brine's maximum temperature will be less than 100^{o}C. Atmospheric pressure steam generated from natural gas, waste heat or solar thermal energy can then be used to directly heat the brine to its maximum temperature (i.e., the top section of the DG system is flooded with steam, which condenses on the exposed brine, raising its temperature towards 100^{o}C). It is also possible to use steam extracted from an intermediate turbine stage of a steam power plant.

[1] When a thermal distillation plant is driven by steam, its Gain Output Ratio (GOR) is the pounds of water produced per pound of steam consumed.

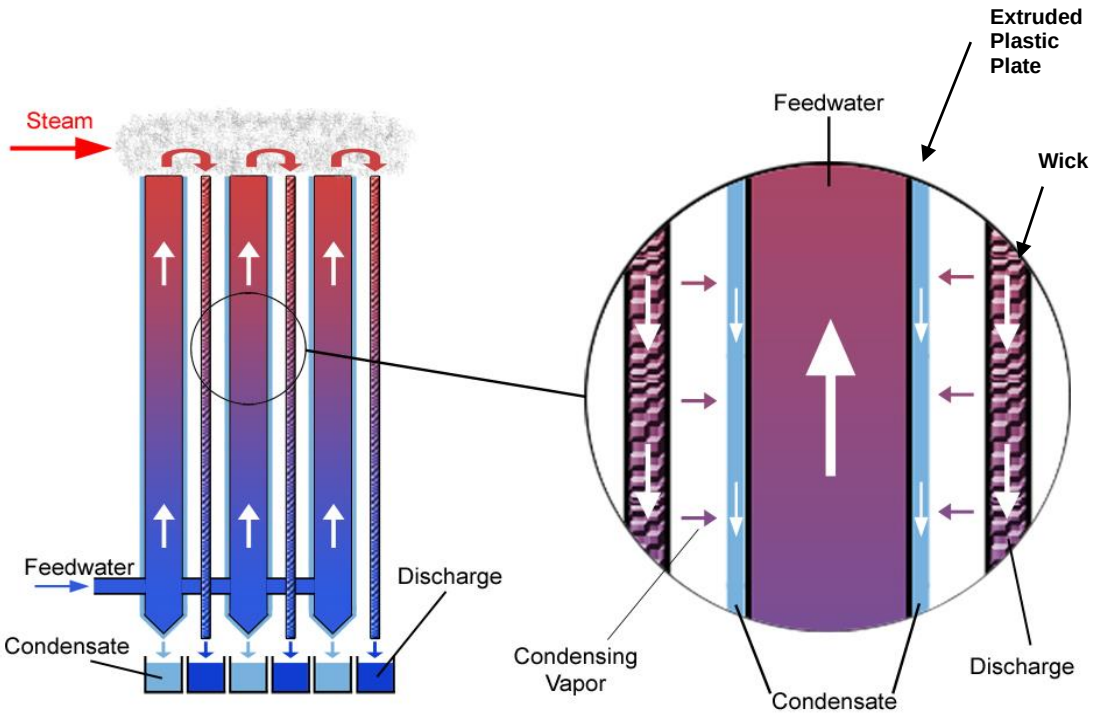

Figure 1 - Schematic of a Diffusion-Gap System

The brine flowing in the wicks will cool and become more concentrated as water evaporates from it. However, the downward flowing brine will always be slightly hotter than the upward flowing brine in the section of plate directly across from it. This temperature difference provides the driving force for water vapor to move from the wick to the cooler plate where it condenses. The cooled brine flowing off the wicks and the condensate flowing off the plates are collected in separate troughs.

Unlike conventional thermal separation processes such as multiple-effect boilers and multi-stage flash evaporation, the DG cycle operates at atmospheric pressure. This has the advantage that the large vacuum vessels of conventional systems are avoided. Since the partial pressure of the water vapor in the gaps between the plates and the wicks is always less than one atmosphere, the water vapor must diffuse through a background of air. By keeping the air gap very small and by including a large amount of surface area (which is economically feasible because the surface area is inexpensive plastic), the DG cycle can have both a high GOR and output.

Many of the humidification/dehumidification (HD) cycles proposed by others have the same advantages as the DG cycle: operation at atmospheric pressure and use of plastic heat exchangers. However, alternative HD cycles do not place the evaporating and condensing surfaces in close proximity as is done in the DG cycle. Fans are sometimes used to circulate air between the evaporating and condensing sections, which leads to high requirements for electrical power, or natural circulation is used, which leads to relatively low fluxes of water vapor (and correspondingly large sizes and/or low efficiencies).

The Operation of a 15-Plate Model

The single-gap proof-of-concept apparatus built under Phase I was used to test the diffusion gap desalination concept. Results from Phase I indicated high efficiencies corresponding to model predictions. However, proportionally large heat losses from this model resulted in a large degree of uncertainty in test results.

The first task under Phase II was to build a scaled-up prototype unit that reduces heat losses and verifies performance predictions. The prototype tested during Phase I had a single diffusion gap, with an active area of 620 cm^2 (0.66 ft^2). The scaled-up unit constructed for Phase II has 30 gaps (15 condenser plates) with an active area of 4.3 m^2 (46 ft^2). Feedwater enters the plates through a manifold at the base, and flows up through the condenser plates. At the top of the plates, the feedwater flows out into a wick, which is heated by direct contact with a heater plate. The hot feedwater flows down both sides of the evaporator surface to a sump at the base. The plates are extruded polyphenylsulfone (PPSU), a polymer with high temperature and moisture resistance. Fiberglass (Garolite G10) plate coated with a wicking polyester flock is used for the evaporating surface. The condensing plates and evaporating surfaces are held in place with a gap of 2.3 mm (0.09 in.) using plastic combs on either side. Figure 2 shows the 15-plate prototype with the plastic comb spacers.

Temperatures of the feedwater, outflow, and condensate were measured with thermistors. Eighteen fine-wire type T thermocouples were used to measure temperature profiles at the top of the plates, vertically along the case, and through the insulation. Tip-bucket rain gauges (NovaLynx 260-2501) measured the outflow and condensate. The heat input was measured with a power transducer (Ohio Semitronics PC5).

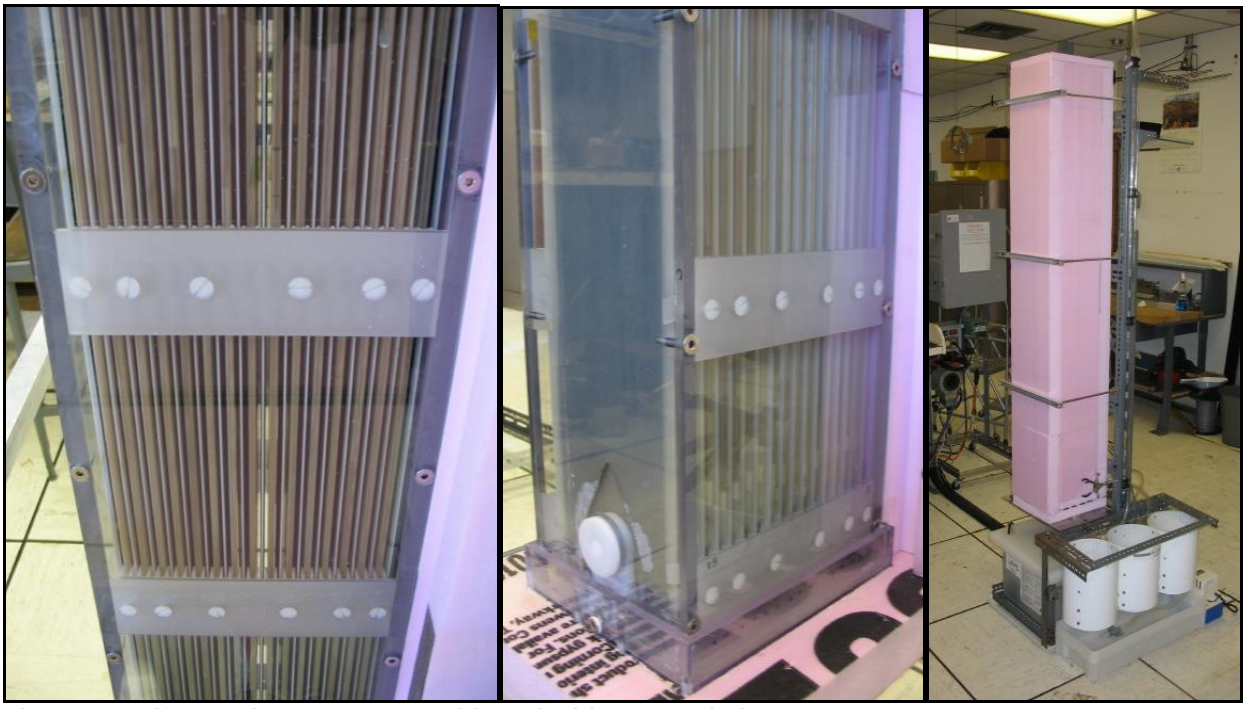

Figure 2 - Fifteen-plate Prototype with and without Insulation

Two series of experiments were conducted to examine the performance over a range of (1) flow rates and (2) maximum temperature (temperature of the feedwater as it enters the top of the evaporator surface). These two parameters have the strongest influence on desalination performance. The first series of tests varied the feed flow rate from 150 ml/min to 400 ml/min, keeping the maximum temperature constant at about 97°C. Each test was allowed to reach steady state; the average steady state performance results are shown in Figure 3. Figure 4 summarizes the second set of tests in which the maximum temperature was varied from 68°C to 98°C, while keeping the flow rate constant at 250 ml/min. Tap water was used for both sets of tests.

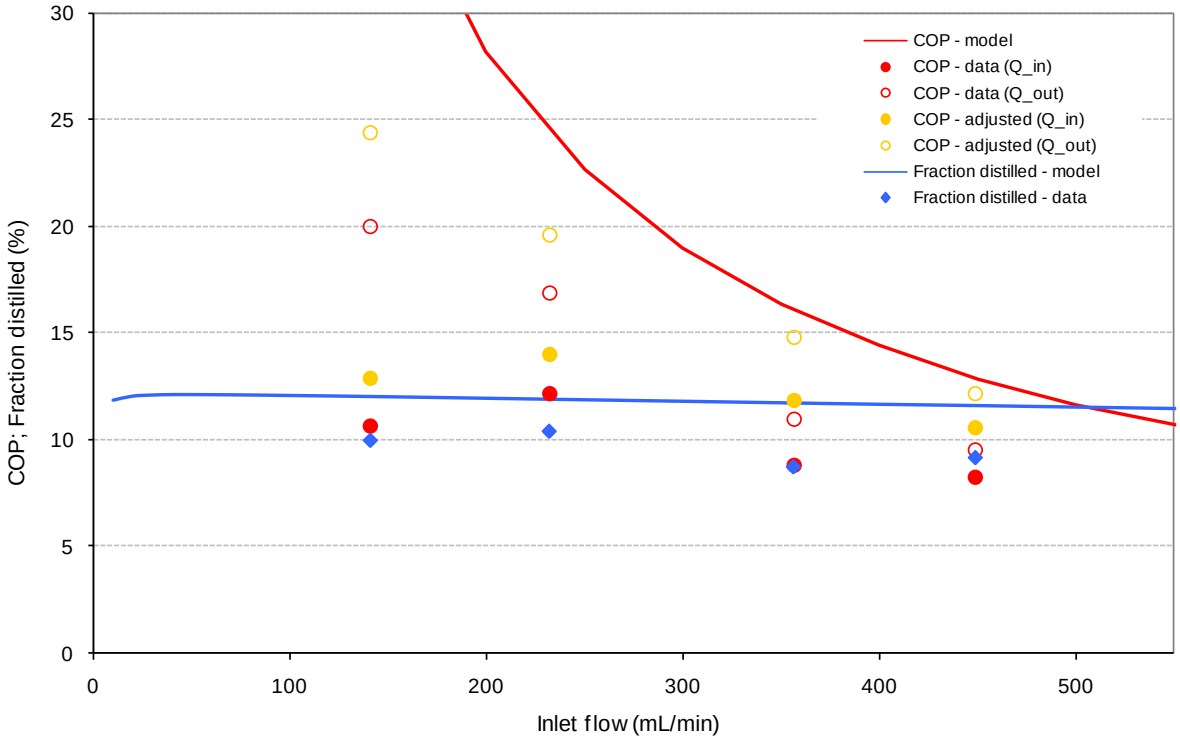

Figure 3 - Performance of 15-plate Prototype with Varying Flow Rates.

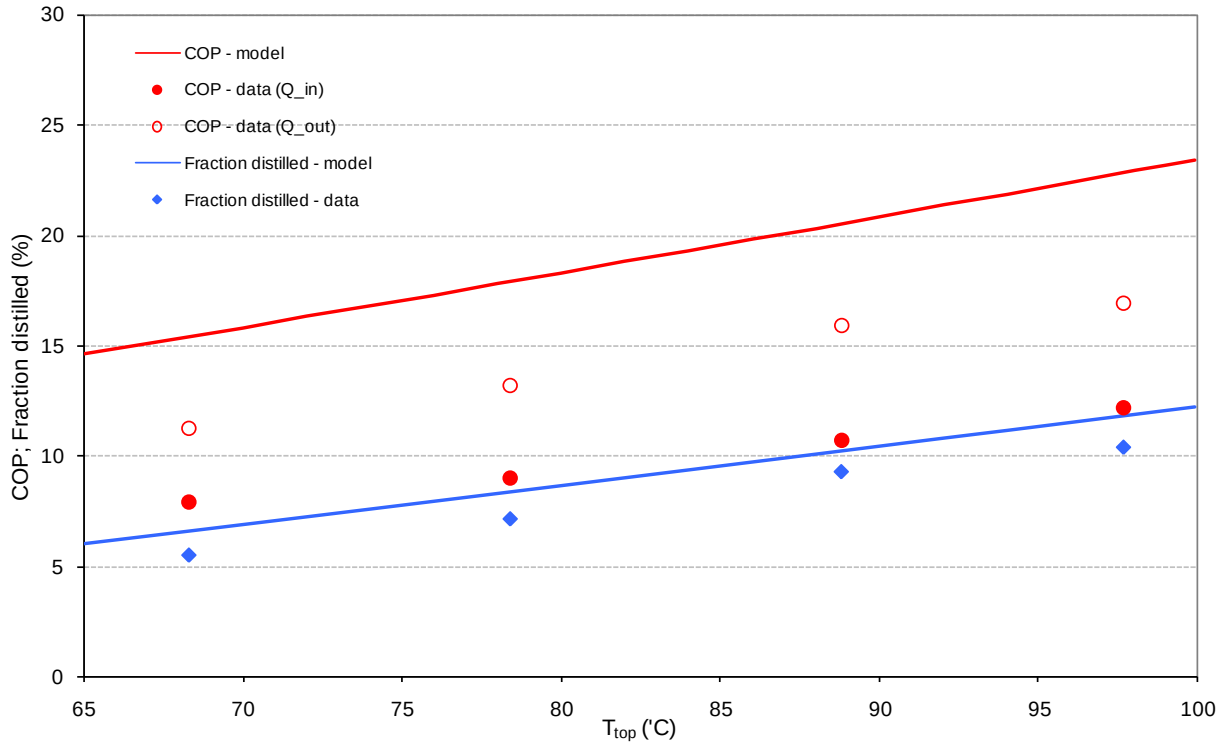

Figure 4 - Performance of 15-Plate Prototype with varying Maximum Temperature

The coefficient of performance (COP) shown in Figure 3 and Figure 4 is given by the latent heat of the distillate divided by heat input. The solid red points are calculated using the electric power drawn by the heater as the heat input. This has a maximum value of about 12.5 for 250 ml/min and T_{max} = 97°C. This doesn't account for heat losses (about 25 W at T_{max} = 97°C), and therefore provides a low estimate for the performance. A more accurate estimate of performance is obtained by subtracting losses from the heat input, i.e. using the energy leaving the apparatus in the outflow streams for the COP calculation. This COP value is shown in Figures 3 and 4 as red circles, having a maximum value of 20 for 150 ml/min and T_{max} = 97°C.

Distillate yield was lower than predicted for all tests, indicating that some of the product was lost into the feed stream. This was confirmed visually: some condensate crossed over to the evaporating surface at points where the gap between plates was reduced to about 0.05 in. due to warping of the plates. The orange points on Figure 3 show an estimate of COP values possible if the loss of condensate was eliminated.

Performance of the 15-plate prototype was lower than the model predictions, but still within 10% of the model for higher flow rates. The tests demonstrate the high performance that can be achieved by scaling up the unit size and thereby reducing heat losses. Additional conclusions regarding the design of the plate assembly include:

1. **Plate Spacing** – With a very tight plate spacing (gap of 2.3 mm, 0.09 in.), even small distortions of the plates can narrow the gap to mix the condensate and feedwater flows. Options for addressing this problem include (a) a larger gap, (b) spacer elements in between the two surfaces, and (c) surface treatment of the condensing plate to avoid drop-wise condensation.

2. **Plate-to-plate flow distribution –** Plate-to-plate temperature distributions indicated that there may have been significant non-uniformity in the distribution of flow between evaporator surfaces. Better uniformity could be achieved by feeding each evaporating surface directly from a single condenser plate, rather than from a combined heater pool.

3. **Air bleed –** Any air dissolved in the feedwater is forced out of solution as the feedwater heats up within the condenser plates. This air forms bubbles which can slow or block flow in individual channels (flutes), if they are not allowed to escape. The 15-plate assembly has a heater block pressed up against the condenser plate outlet, hindering air bubbles from escaping.

Design for Manufacturing

Results from the 15-plate prototype were used to redesign the plate assembly to use low-cost materials and standard manufacturing methods. The revised design is shown in Figure 5. The flocked rigid evaporator plate is replaced by a tubular fabric sleeve that fits over every second plate. The plates are constructed from low-cost polypropylene extrusion (2 mm profile extrusion supplied by Coroplast), with solid polypropylene edge molding strips to support the fabric. The fabric is a knit nylon, slightly undersized and stretched to keep it tight over the plate. Silicone spacers are also used to keep the fabric in place.

Figure 6 shows the details at the top of the plate. Water flows out of the flutes into a single header space at the top of the plate, and from there flows out through holes in one side to a fabric distributer pad. The distributer pad transfers the flow onto the fabric sleeve, and is supported by a strip of folded film, which prevents flow from reaching the condensing surface. The plates are designed for steam heating: the mesh at the top of the sleeve allows for better contact between steam and water flowing out onto the distributer pad.

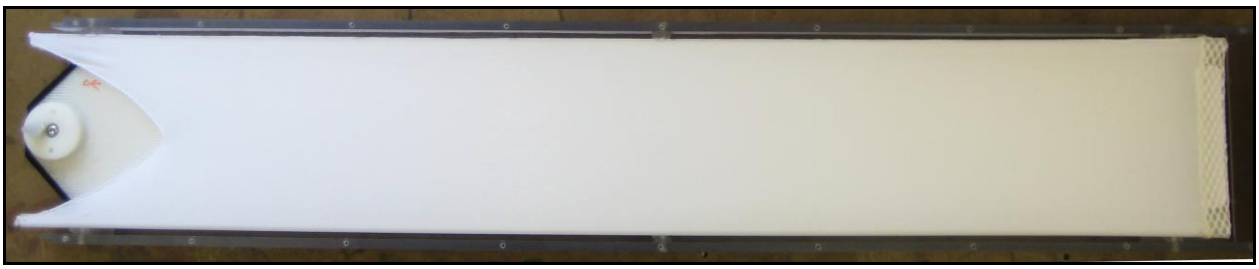

Figure 1 - Plate assembly, with fabric sleeve stretched over polypropylene plate.

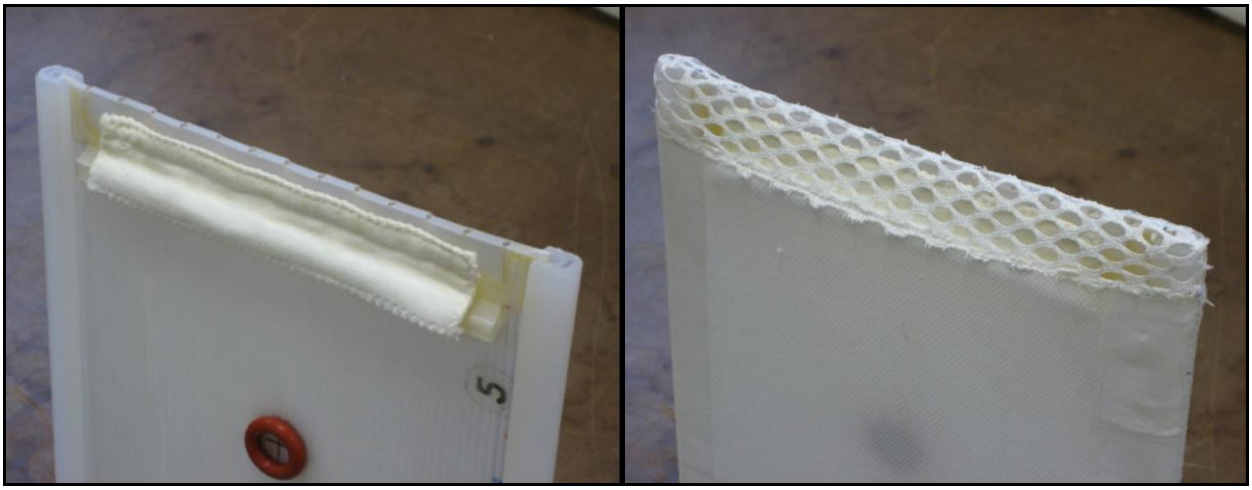

Figure 6 - The top of a plate: (a) without fabric sleeve, showing an o-ring spacer, polypropylene edge strips, and fabric distributer pad; (b) with fabric sleeve in place, showing the mesh section.

Initial experiments were conducted to test performance in between design changes. Figure 7 shows the change in performance for a given flow rate and temperature. Several important observations from these results are:

1. The most noteworthy improvement was in the second modification: adding strips of silicone along either side of the sleeve to direct the flow. This change prevented the heated water from flowing along the edge molding pieces, where it is not involved effectively in the latent heat transfer.

2. The inlet distributer tube added to the plate inlet manifold as the first modification had little effect on performance. This was confirmed by later returning to the old plates, using them together with the improved sleeves. As shown by modification 4 in Figure 7, the performance was similar to the new plates.

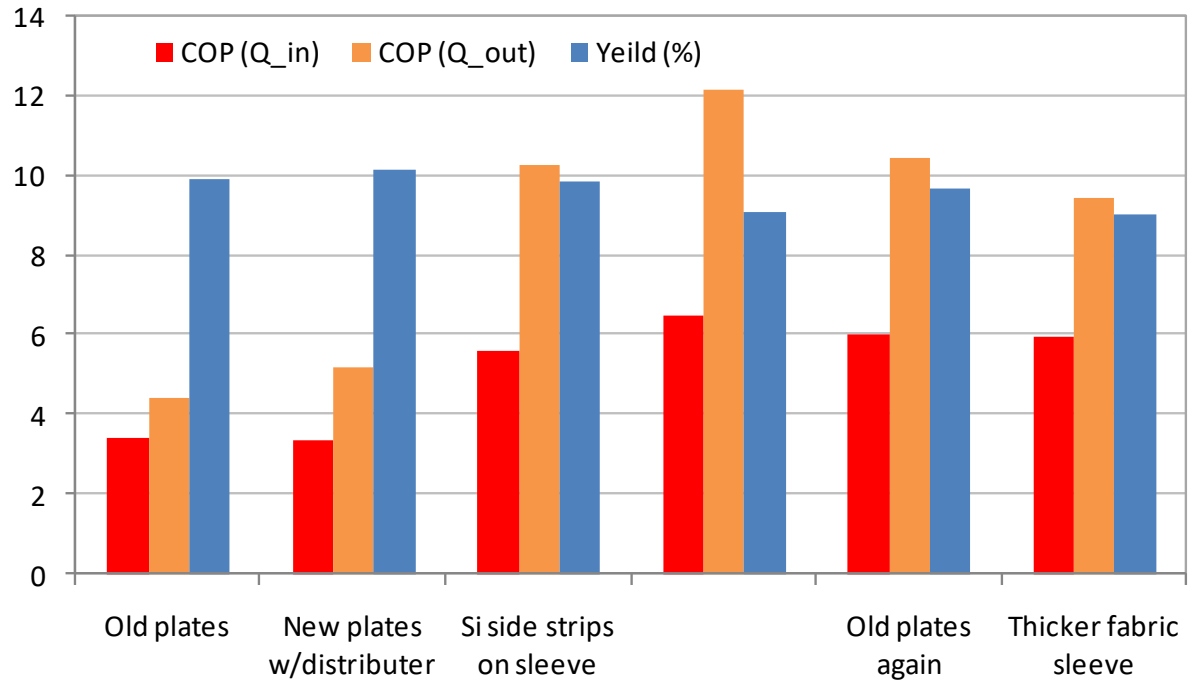

Figure 7 - Desalination performance with changes to the plates and sleeve construction. All tests were done with approximately 100 ml/min flow and 93°C maximum fluid temperature.

3. The thicker sleeve material did not seem to have a significant effect on performance. However, this test involved another modification: using heat-activated polyester adhesive for the side strips instead of silicone. The polyester adhesive did not fully impregnate the fabric, and so was not fully effective in preventing flow along the polypropylene edge supports.

Figure 8 shows the results of further testing with the silicone side strips, at different flow rates. Both the yield fraction and COP are below the model predictions. Yield data is approximately 5% low, which may be due to condensate loss (perhaps flowing off at the edge molding pieces instead of down to the center of the plate).

For all four flow rates shown in Figure 8 the heat losses ($Q_{in} - Q_{out}$) were between 25 and 30 W. For the 50 ml/min case, the heat input was 37 W and the losses 25 W. With such relatively large heat losses, the uncertainty on the COP calculation is large.

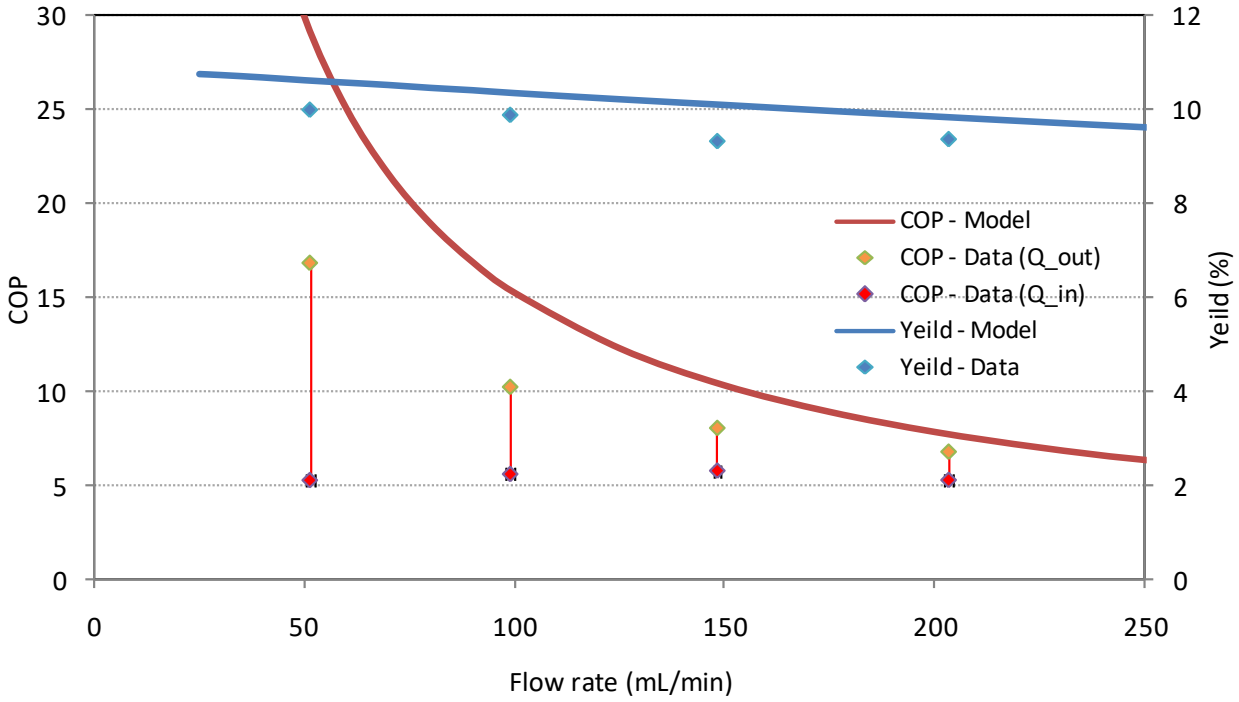

Figure 8 - Performance of the 6-plate unit with varying flow rates, with computer model predictions for reference. The maximum temperature was constant at approximately 93°C.

The six-plate unit was tested with sea water with increasing salinity, up to 12%, with results shown in Figure 9. All the tests re-circulated the feedwater, mixing both condensate and brine out-flows back into the feed tank. For higher salinity test, dry sea salt was added to achieve the desired salinity.

As with the tests using tap water, the yield fractions shown in Figure 9 are slightly lower than model predictions, ranging from approximately 5% to almost 10% low for the highest salinity. The COP dropped off significantly between the 3.5% and 5.6% salinity tests, but then was relatively constant for higher salinity levels. These results differ significantly from model predictions and should be verified in later testing.

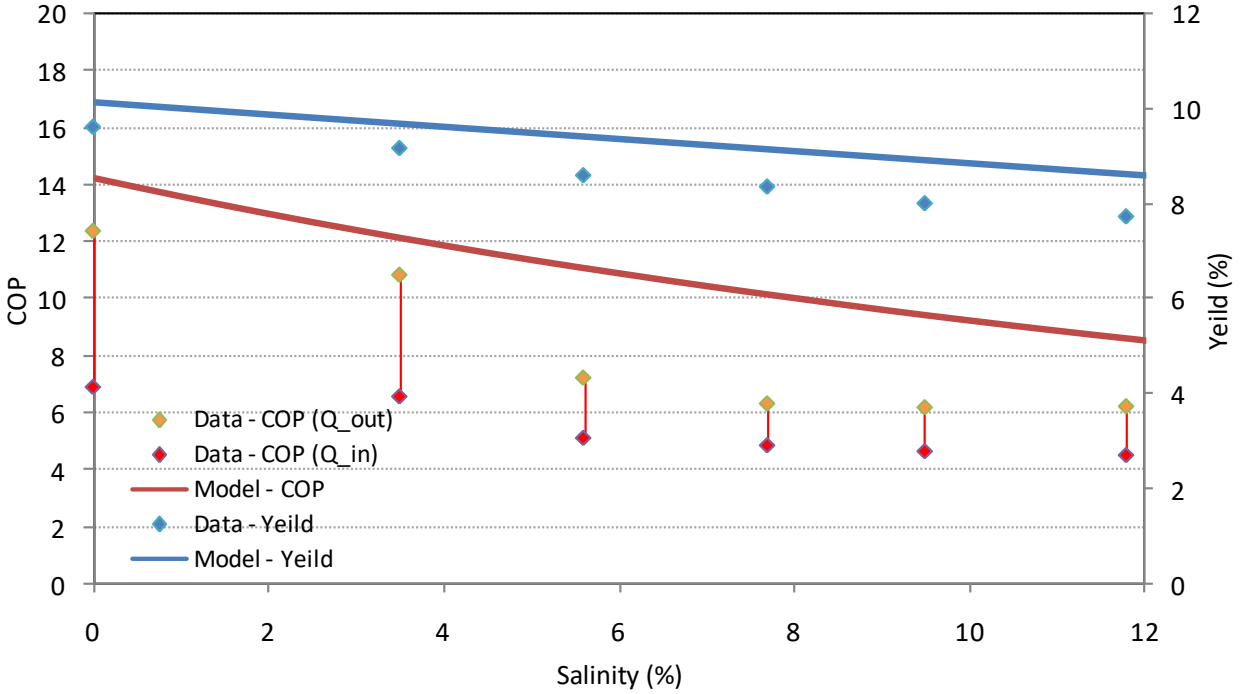

Figure 9 - Performance with varying feedwater salinity levels. (The flow was constant at approximately 100 ml/min, and the maximum temperature 93°C).

3.0 Solar Collector – Work Completed

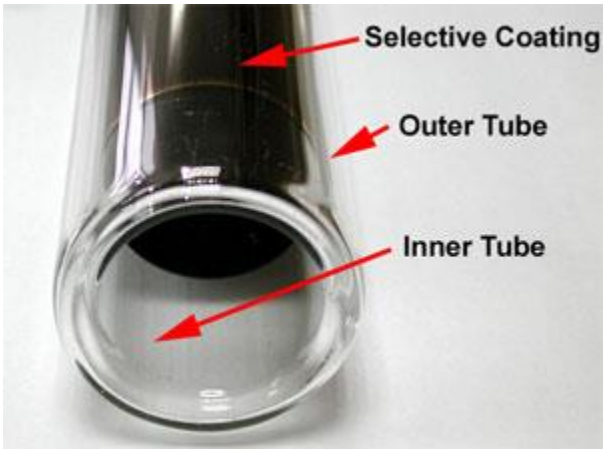

Figure 10 – Evacuated-Tube Dewar-Type Solar Collector

The Dewar-Tube Steam-Generating Collector

The second important objective of the work reported here is to develop a low-cost solar collector that can provide the thermal energy needed by the desalination system. As shown in Figure 10, the developed collectors use double-wall Dewar tubes (essentially vacuum bottles). Each tube is 180 cm in length, and has outer and inner diameters of 5.8 cm and 4.7 cm, respectively. The inner walls of these tubes have a selective absorber coating on the vacuum side that absorbs visible radiation, but doesn't reradiate infrared radiation from the hot absorber surface. Solar collection efficiencies are extremely high and stagnation temperatures (i.e., operation without the tubes delivering heat) can exceed 400^{o}F. These tubes are now manufactured in very high volume in China and they can be purchased in the U.S. in quantity for approximately $4 per square foot of absorber area.

For the solar desalination system, the solar source of thermal energy uses the Dewar-tube collectors as simple steam generators. As shown in Figure 11, an array of Dewar tubes is mounted on a level frame. Each tube is connected to a manifold that is fed mineral-free condensate from the output of the desalination plant. The level of water in the manifold determines the level of water within each tube. At typical operating conditions, steam is quiescently generated from the free surface of water within the tubes as the tubes absorb solar radiation. The steam is collected in the same manifold that delivered water to the tubes.

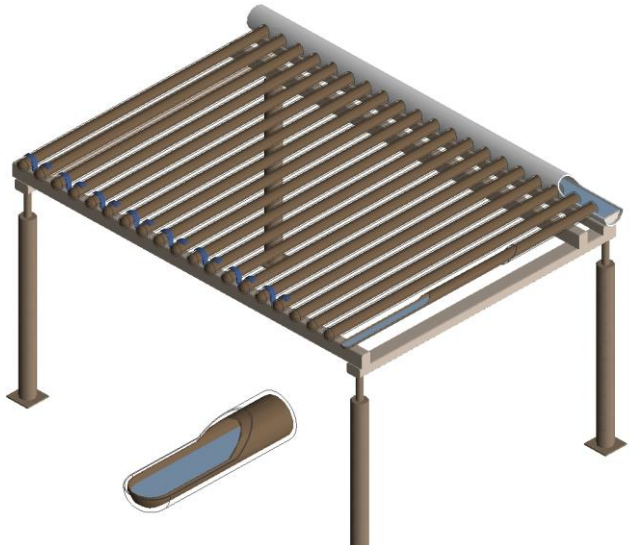

Figure 11 – 20-Tube Dewar-Tube Solar Array that Directly Generates Steam

It is important to note that transferring energy as the latent heat of steam is very effective and the flow rates of water to the solar collectors are very low. At peak solar insolation, each tube supplies approximately 165 Btu/h steam, which is equivalent to an inlet water flow to the tube of 0.02 gph. Assuming 20 tubes are served by a common steam/water manifold, the feedwater flow is 0.4 gph. For a 5" diameter manifold, the maximum steam velocity is very low: 11.1 ft/min. These low water and steam velocities allow a single manifold to be used for both flows.

Operation of the 24-Tube Solar Collector

Following a small-scale test conducted in Phase I, a larger demonstration collector was constructed and tested during the 2008 summer. The unit consists of 24 evacuated collector tubes oriented horizontally, and half filled with water. The central manifold supplies tubes with water and directs the steam out. Figure 12 shows the collector during a test. Tube supports were constructed with polyisocyanurate insulation foam, and the manifold was insulated with 38 mm (1.5 in.) of polyisocyanurate foam. The total absorber area was 1.9 m^2 (20.5 ft^2), and the gross collector area was 4.5 m^2 (48 ft^2).

In testing the collector this steam produced was condensed and measured using a tip-bucket rain gauge (NovaLynx 260-2501). Ambient temperature and temperatures inside the manifold and collector tubes were measured with sealed thermistors (except for 2 type K thermocouples, which were used to measure the tube surface temperature and the temperature of the steam just below the surface). Both total and diffuse insolation levels were measured with Li-Cor 200 pyranometers.

A summary of the results of steam generation from distilled water are shown in Figure 3. The efficiency is given by the energy value of the steam generated (including preheat, phase change,

Figure 2. 24-tube collector used for direct steam generation, during testing in 2008.

and superheat components) over the solar radiation absorbed by the collector tubes. The radiation absorbed by the tubes is calculated using incidence angle modifiers for both beam and diffuse radiation. It does not include corrections for radiation reflected from the white backplane. An indication of the effectiveness of the white reflective backplane is given by the 6/21 data point shown in Figure 3; during this test day, the backplane was covered with a matte black cover.

The collector heated up and generated steam on all the test days during the 1½ month test period. Data in Figure 3 indicates a clear relationship between radiation and efficiency that is not affected greatly by patterns of insolation, such as variations in cloud cover or haze. The results were also not greatly affected by the water level within the tubes. The blue data points shown in Figure 3 represent days in which the water level was kept at 1/3 full rather than the normal 1/2 full level. The red data points represent days in which the water level was maintained by a weir, as opposed to simply pumping back in all the condensed steam. The weir method was not as effective in maintaining a uniform water level, but allowed the level to drop toward the middle of the day.

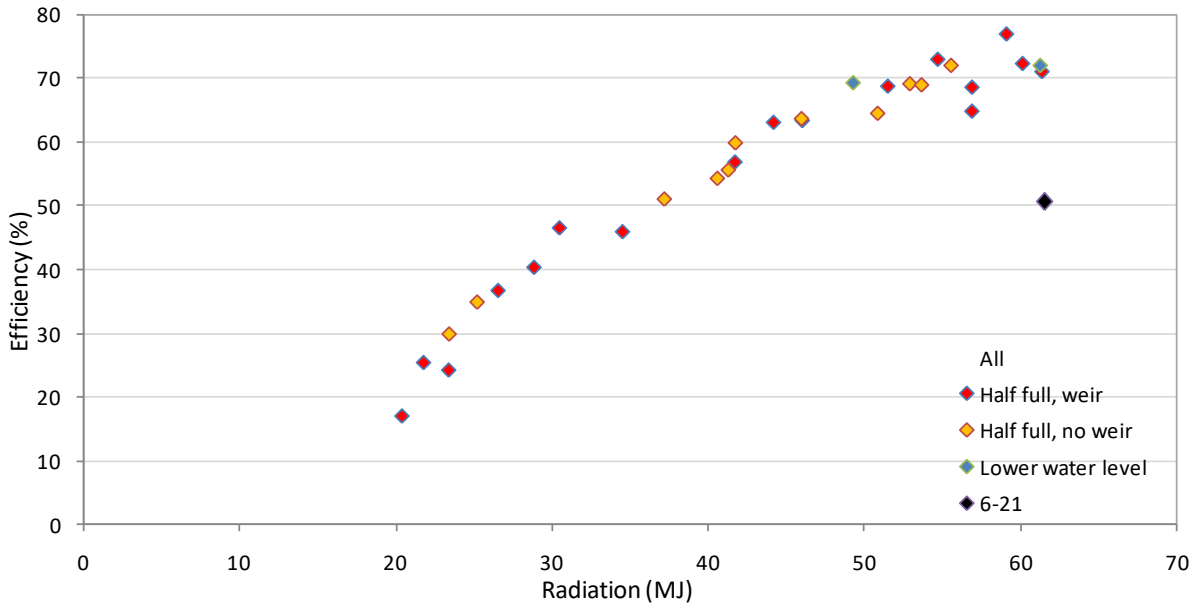

Figure 3 - Efficiency of the 24-tube collector in steam generation, with colored data points indicating variations in tube fill level. Data represents a variety of weather conditions from 6/17/2008 – 7/31/2008.

Data for a typical day of full sun is shown in **Figure 4**. The measured total and diffuse insolation levels match theoretical clear sky models for the day, except for some extra reflection in the morning and a few clouds. The condensed steam flow peaks at about 45 ml/min, which represents an energy output of 1.65 kW. The equivalent instantaneous efficiency, calculated as described above, is just over 90%. Calculating the efficiency based on the total radiation incident on the gross collector area would give an instantaneous efficiency of 39%.

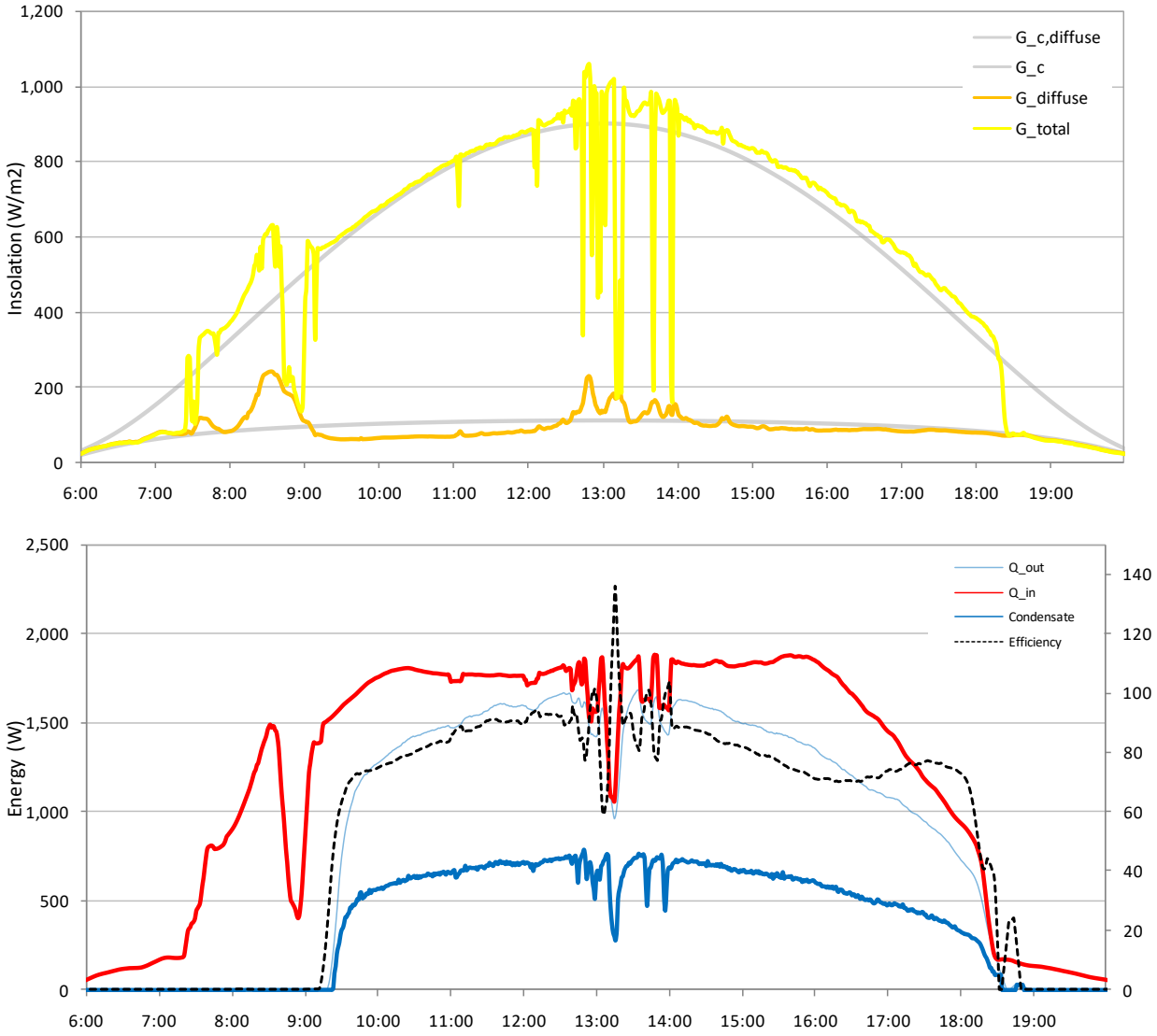

Figure 4. Data for 7/2/2008, showing insolation levels and collector performance for a full sun day.

4.0 Conclusions

An array of steam-generating solar collectors driving a DG desalination unit can meet future needs for sustainable sources of potable water. The technology will be most useful where reverse osmosis in not acceptable either because (1) the cost of electricity is too high, (2) the feedwater has contaminants that would foul the membranes of the reverse-osmosis system, or (3) the application requires water purity that cannot be met by reverse-osmosis.

DG desalination has the potential to be more efficient that the thermal desalination technologies now in use (i.e., multi-stage flash evaporation and multiple-effect distillation). Whereas thermal desalination technologies now operate at GORs on the order of 9 to 11, a laboratory DG model demonstrated the potential to increase GORs to between 15 and 20.

The cost of water from a thermal desalination plant that is driven primarily by solar energy will be strongly influenced by the cost of the solar thermal collectors. The steam-generating solar thermal collectors that were developed in this project have demonstrated a solar collection efficiency comparable to the evacuated-tube solar collectors now on the market. This high efficiency is achieved in a simple design that avoids the metallic internal heat exchangers that are an integral part of conventional evacuated-tube collectors. Manufacturing costs for the steam-generating collectors can be half that of conventional evacuated-tube collectors.

Both the steam-generating solar collector and the DG desalination system must prove their ability to operate efficiently in the field for relatively long periods of time at a scale that is at least ten times larger than the models tested in this project. The maintenance requirements and expected lifetimes for the technologies must be determined from these field operations. Field operation of a DG desalination system using steam-generating solar collectors is the logical next step in the commercialization of this technology.